ORGANIC CHEMISTRY

Organocatalyzed atroposelective dynamic kinetic resolutions via transient seven-membered cyclic hemiacetals

Qinglong Zhou[1]†, Yuhang Chen[1]†, Wei Yuan[1]†, Sai Vikrama Chaitanya Vummaleti[2]†, Xinyue Xiang[1], Bowen Zhu[1], Yonggui Robin Chi[3]*, Xinglong Zhang[4,2]*, Xing Yang[1]*

Catalytic atroposelective dynamic kinetic resolution via the formation of transient bridged biaryl intermediates represents an expedient route for the synthesis of axially chiral biaryls. Progress in this field has been limited to the reactions promoted by bridged biaryl intermediates with five- or six-membered rings. Herein we demonstrate the first example of a carbene-catalyzed atroposelective dynamic kinetic acylation reaction via transient seven-membered cyclic hemiacetals. The key for the success of this reaction relies on the formation and configurational instability of the transient seven-membered cyclic hemiacetal intermediate. The axially chiral biaryl aldehyde products obtained via this method can undergo a series of further transformations. Notably, one of the axially chiral biaryl aldehyde products can be used as the key and common intermediate for the asymmetric synthesis of natural product steganone. Preliminary density functional theory calculations reveal the molecular origins underlying the observed chemo- and enantioselectivity outcomes.

INTRODUCTION

Axially chiral architectures, especially biaryl-based atropisomeric architectures, are increasingly encountered in modern materials, bioactive molecules, natural products, and privileged chiral catalysts or ligands (*1*–*5*). Therefore, asymmetric synthesis of biaryl atropisomers has attracted substantial attention from chemists (*6*–*11*). Among numerous reported methods, the atroposelective dynamic kinetic resolution (DKR) involving ring manipulations of configurationally labile bridged biaryls stands out as a cutting-edge technology for the construction of atropisomeric biaryls (*12*–*15*). The key to the success of these reactions is the rapid racemization of the bridged biaryls (Fig. 1A), as well as hydrogen bond–assisted racemization (*16*). Overall, the atroposelective DKR involving ring manipulations can be categorized into two types: (i) DKR of configurationally labile bridged biaryls (type I) and (ii) DKR via the formation of configurationally labile bridged biaryl intermediates or transition states (TS) (type II). For the former category, substantial advancements have been made in the dynamic kinetic ring–opening reactions of bridged biaryls containing five- (*17*–*24*) or six- (*25*–*32*) membered rings, since Bringmann reported the lactone strategy for the atroposelective synthesis of axially chiral biaryls (*25*). Recently, our group reported an organocatalyzed dynamic kinetic hydrolytic ring–opening reaction of seven-membered bridged biaryls (*33*). For the latter category, the racemization usually required the interaction between heteroatom-containing functional groups and unsaturated carbonyls to form transient configurationally labile bridged biaryl intermediates. Many elegant DKR reactions have been developed via the formation of transient five- (*34*–*37*) or six- (*38*–*52*) membered bridged biaryl intermediates as reported by Akiyama (*38*), Wang (*39*–*41*), Hornillos and Lassaletta (*42*), Chi and Jin (*43*, *44*), Fu (*45*), Cheng (*35*, *36*), and Wang (*37*), or TS through Lewis acid–base interaction as pioneered by Hornillos and Lassaletta (*35*, *49*–*52*), Clayden (*46*), and Wang (*47*). However, the DKR reaction involving the formation of bridged biaryl intermediates with larger ring size, such as seven-membered bridged biaryl intermediates, remains underdeveloped and challenging. The main challenge deals with the racemization issue of the bridged biaryl intermediates with larger-sized rings (*53*). From five-, six-, to seven-membered bridged biaryl intermediates, the angles around the axis in the racemization TS become smaller, which leads to an increase for the rotation barrier such that the racemization becomes more slowly, making highly atroposelective DKR reaction more difficult.

Our group is interested in the organocatalyzed asymmetric synthesis and the conversion of bridged biaryls (*33*, *54*, *55*). Herein, we reported a carbene-catalyzed (*56*–*62*) atroposelective DKR via the formation of transient seven-membered cyclic hemiacetals (Fig. 1B). The key to the success of this reaction is the formation and configurational instability of the transient seven-membered cyclic hemiacetal intermediate. In addition, the carbene-catalyzed atroposelective acylation process is also important, which afforded a series of axially chiral biaryl aldehyde products in high yields with excellent enantioselectivities. Notably, one of the axially chiral biaryl aldehyde products can be served as a key and common intermediate for the asymmetric synthesis of natural product (steganone) (*63*–*71*). In previous works, to obtain this key intermediate, the use of stoichiometric chiral sources [chiral pool (*66*–*68*), chiral auxiliary (*69*, *70*), and chiral reagent (*71*)] and multistep synthesis are required. Herein, we can achieve the catalytic asymmetric synthesis of this key intermediate in two steps with a higher yield, which highlights the importance of this work.

[1]Key Laboratory of Chemical Biology and Traditional Chinese Medicine (Ministry of Education of China), Key Laboratory of the Assembly and Application of Organic Functional Molecules of Hunan Province, College of Chemistry and Chemical Engineering, Hunan Normal University, Changsha 410081, P. R. China. [2]Institute of High Performance Computing, Agency for Science, Technology and Research (A*STAR), Singapore 138632 (Singapore). [3]School of Chemistry, Chemical Engineering, and Biotechnology, Nanyang Technological University, Singapore 637371, Singapore. [4]Department of Chemistry, The Chinese University of Hong Kong, Shatin New Territories, Hong Kong, P. R. China.
*Corresponding author. Email: xingyang@hunnu.edu.cn (X.Y.); xinglong.zhang@cuhk.edu.hk (X.Z.); robinchi@ntu.edu.sg (Y.R.C.)
†These authors contributed equally to this work.

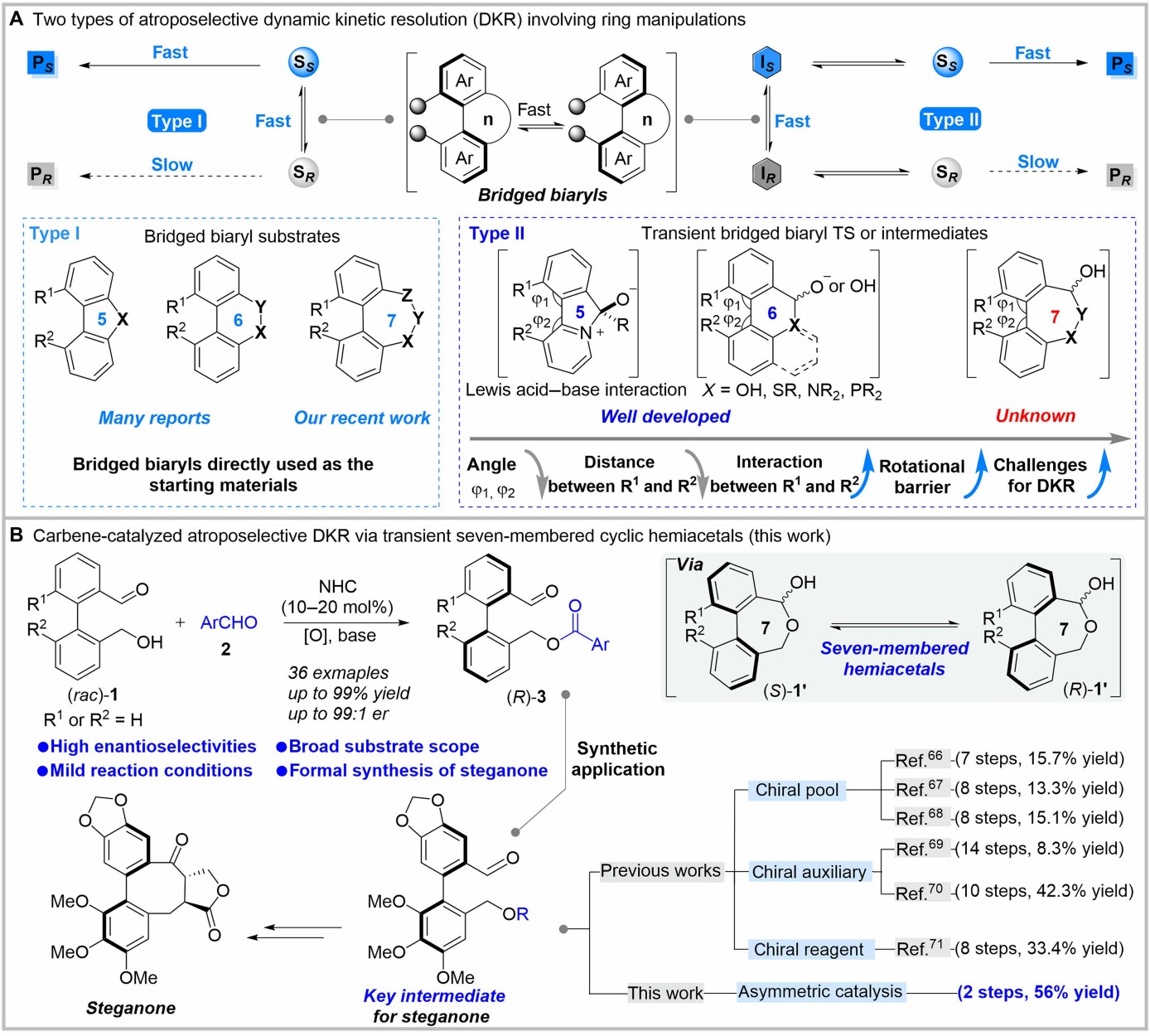

Fig. 1. Atroposelective DKRs involving ring manipulations. (**A**) Two types of atroposelective dynamic kinetic resolution (DKR) involving ring manipulations. (**B**) Carbene-catalyzed atroposelective DKR via transient seven-membered cyclic hemiacetals.

RESULTS

Reaction condition optimization

We initiated our studies using biaryl hydroxyl aldehyde **1a** and 2-naphthaldehyde **2a** as the model substrates in the presence of a tetra-tert-butyldiphenylquinone (DQ) (*72*) oxidant searching for appropriate conditions, with Table 1 summarizing the main results. The enantiomerically enriched axially chiral biaryl aldehyde product **3a** was smoothly formed with promising enantiomeric ratio (er) value using an aminoindanol-derived precatalyst with a *N*-mesityl substituent (**A**) (*73*) and examined by using DIPEA as the base and DCM as the solvent (Table 1, entry 1). Replacing the *N*-mesityl unit of **A** with an electron-deficient trichlorophenyl group (**B**) (*74*) gave the product in 52% yield and 57:43 er (Table 1, entry 2). The side product biaryl seven-membered lactone **4** was detected when a precatalyst (**C**) (*75*) with a more electron-deficient *N*-pentafluorophenyl substitute was used, and the ratio of target product **3a** to side product **4** is 2:1 (Table 1, entry 3). Satisfactory, the reaction enantioselectivity was notably improved when using catalyst **D** (Table 1, entry 4) (*76*). Thereafter, when phenylalanine-derived catalyst **E** (*77*) was used, the product was obtained in good yield and enantioselectivity, and the ratio of target product **3a** to side product **4** is >20:1 (Table 1, entry 5). The reaction solvent proved to be essential to the reaction enantioselectivities (Table 1, entries 6 to 9), and the solvent 1,2-dichloroethane (DCE) was demonstrated to be the best choice in terms of both yields

Table 1. Optimization of the reaction conditions. General conditions: 1a (0.10 mmol), 2a (0.12 mmol), NHC precursor (0.02 mmol), base (0.1 mmol), 4-Å MS (100 mg), DQ (0.12 mmol) and solvent (2.0 ml), 72 hours.

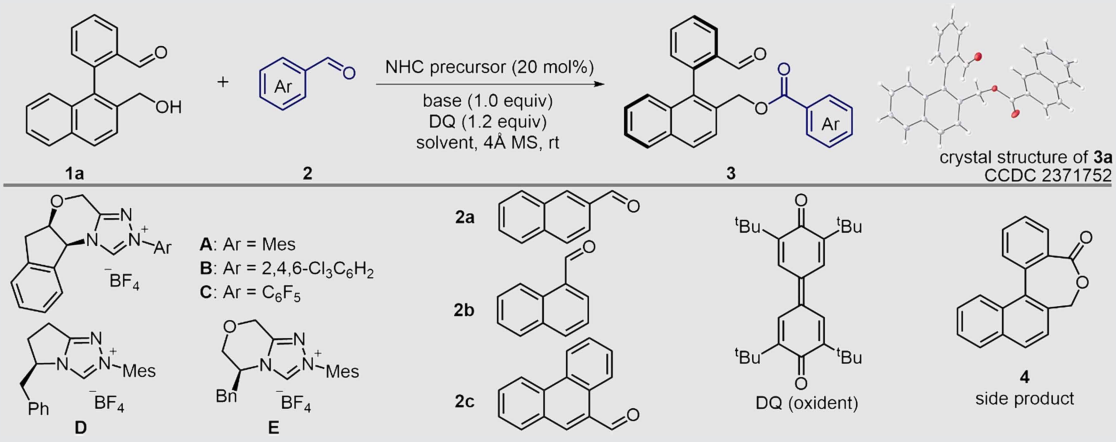

Entry	NHC precursor	Solvent	Base	Yield[§] (%)	3:4[¶]	Er[#]
1	A	DCM	DIPEA	54	>20:1	68:32
2	B	DCM	DIPEA	52	>20:1	57:43
3	C	DCM	DIPEA	37	2:1	61:39
4	D	DCM	DIPEA	52	>20:1	84:16
5	E	DCM	DIPEA	82	>20:1	90:10
6	E	Toluene	DIPEA	70	>20:1	50:50
7	E	THF	DIPEA	65	>20:1	53:47
8	E	$CHCl_3$	DIPEA	60	>20:1	67:33
9	E	DCE	DIPEA	85	>20:1	91:9
10	E	DCE	Cs_2CO_3	95	>20:1	87:13
11	E	DCE	K_2CO_3	80	>20:1	88:12
12	E	DCE	DBU	60	>20:1	57:43
13	E	DCE	LiOH	62	>20:1	92:8
14*	E	DCE	LiOH	89 (94)**	>20:1	94:6
15*†	E	DCE	LiOH	90 (85)**	>20:1	94:6
16*‡	E	DCE	LiOH	90 (94)**	>20:1	96:4

*LiOH (0.3 mmol); †2b instead of 2a; ‡2c instead of 2a; §NMR yields using 1,3,5-trimethoxybenzzene as internal standard; ¶determined via NMR; #the er values were determined by HPLC using a chiral stationary phase; **isolated yield.

and enantioselectivities (Table 1, entry 9). The effect of base was evaluated for the reaction system (Table 1, entries 10 to 13), and the results showed that inorganic base LiOH could slightly improve the enantioselectivity (Table 1, entry 13), even if the yield was moderate. Then, we found that increasing the amount of LiOH gave an apparent improvement in yield and enantioselectivity (94% yield and 94:6 er; Table 1, entry 14). The absolute configuration of **3a** was confirmed by x-ray analysis. We next screened different aldehydes (Table 1, entries 14 to 16 and see the Supplementary Materials for details) to further optimize the reaction conditions. Last, when phenanthrene-9-carbaldehyde **2c** was used, the corresponding product **3c** was obtained in high yield and enantioselectivity (94% yield and 96:4 er in Table 1, entry 16).

Substrate scope

With the optimal reaction conditions in hand, we next evaluated the scope of the carbene-catalyzed atroposelective acylation reaction, and the results are shown in Fig. 2. A wide range of biaryl hydroxyl aldehydes were compatible in this reaction, giving the axially chiral biaryl aldehyde products (**3c** to **3am**) in high yields (up to 99%) and excellent enantioselectivities (up to 99:1 er). Initially, this reaction was investigated with a range of biaryls bearing an upper benzene ring and a lower naphthalene ring (**3d** to **3t**). Electron-donating or -withdrawing substituents at the 5- and 4-position of the upper benzene ring were all tolerated, and the chiral aldehyde products (**3d** to **3j**) were isolated in 60 to 99% yields and 93:7 to 98:2 er. Biaryl substrates with fluorine atom at the 3-position of the upper benzene ring underwent the reaction smoothly, with the desired product (**3k**) obtained in 72% yield and 95:5 er. To our delight, switching the phenyl group to a thienyl group, a heteroaryl-containing axially chiral biaryl product (**3l**) was accessed in high yield and er value. In addition, the reaction was carried out with good conversion and enantiomeric induction for a variety of substrates with different

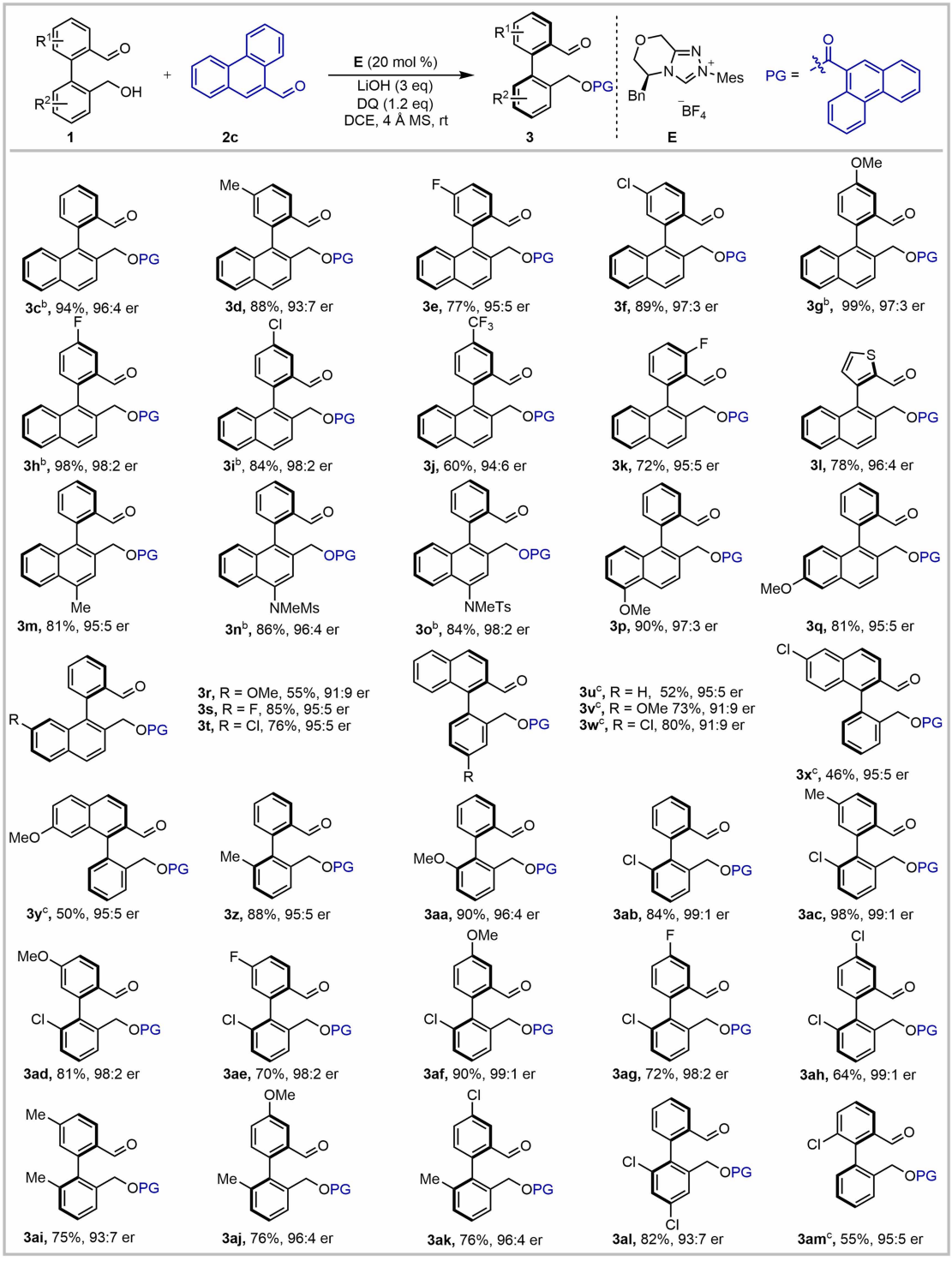

Fig. 2. Substrate scope. Reaction conditions: 1 (0.10 mmol), 2c (0.12 mmol), NHC·HBF_4 E (20 mol%), LiOH (3.0 equiv), 4-Å MS (100 mg), DQ (1.2 equiv), and anhydrous DCE (2.0 ml) was added and stirred at room temperature for 7 days; [b] Reactions for 72 hours; [c]1 (0.10 mmol), 2c (0.12 mmol), NHC·HBF_4 A (20 mol%), LiOH (3.0 equiv), 4-Å MS (100 mg), DQ (1.2 equiv), and anhydrous $CHCl_3$ (2.0 ml) was added and stirred at room temperature for 7 days.

substituents at the lower naphthalene ring (**3 m** to **3t**). Notably, the reaction proceeded smoothly when the naphthalene ring was substituted with basic N-atoms, affording the corresponding products (**3n** and **3o**) in high yields with excellent enantioselectivities. Next, biaryl substrates containing an upper naphthalene ring and a lower benzene ring were investigated. Switching the carbene catalyst **E** to **A**, a series of this type of substrates were converted into the corresponding acylation adducts (**3u** to **3y**) with satisfactory results. Last, we found that the biaryl substrates with two benzene rings were also amenable in the reaction. Installing different functional groups such as methyl, methoxy group and chlorine atom on the 6-position of the lower benzene ring, afforded the target axially chiral biaryl products (**3z** to **3ab**) in high yields and excellent enantioselectivities. Next, a series of substitutes on both upper and lower benzene ring were examined, with desired products (**3ac** to **3am**) formed in consistently good to excellent results.

Synthetic applications

The synthetic utility of this atroposelective dynamic kinetic acylation reaction has been demonstrated by a scale-up reaction, several transformations and the application for the formal synthesis of natural product (steganone). First, we carried out a gram-scale reaction of compound **1a** under a lower catalyst loading (10 mol %), which afforded axially chiral biaryl aldehyde product **3c** in comparable results as the above small-scale reaction (95% yield and 95:5 er, Fig. 3A). Then, several synthetic transformations of compound **3c** were conducted (Fig. 3A). The Wittig reaction of **3c** with the stable ester-bearing ylide resulted in the formation of the target olefin derivative **5a** in 99% yield, 7:1 *E:Z* ratio, and 95:5 er. Oxidation of the aldehyde group could yield axially chiral biaryl carboxylic acid **5b** in good yields and er value. Treatment of **3c** with P-(1-diazo-2-oxopropyl)-dimethyl ester produces alkyne product **5c** in 79% yield and 95:5 er. In addition, axially chiral diol **5d** could be obtained in 99% yield by reducing **3a** with $LiAlH_4$. Both the aldehyde and ester groups in **3c** could be converted into hydroxyl groups (**5e**) through a one-pot, two-step method without loss of enantiopurity. The hydroxymethyl group of **5c** can be further oxidized to an aldehyde group (**5f**), and the enantiomeric excess (*ee*) was maintained. Last, the related dibromo chemical **5g** could be afforded from **5d** in a good yield without erosion of the enantioselectivity. This dibromide can serve as a versatile precursor in nucleophilic substitutions.

We found that our method can be used for the synthesis of a key intermediate in the asymmetric total synthesis of Steganone (Fig. 3B). We started with readily available aryl iodide and arylboronic acid to obtain biaryl hydroxyl aldehyde **6** in 70% yield through Suzuki-Miyaura coupling. Then, the key intermediate **7** was obtained in good yield and enantioselectivity (80% yield and 95.5:4.5 er) via the carbene-catalyzed atroposelective DKR under the above standard conditions. In previous works (*66*–*71*), to obtain this type of axially chiral aldehyde intermediate usually required the use of stoichiometric chiral sources and multistep synthesis. Treatment of **7** with methyl lithium produced **8** in 92% yield, 96:4 er and 3.2:1 diastereomeric ratio (dr). Then, the primary hydroxyl group can be selectively protected by TBSCl to obtained **9** in 80% yield and 95:5 er. On the basis of the reported synthetic route (*64*, *68*, *71*), a formal total synthesis of (+)-steganone could be achieved.

Mechanistic studies

To understand the reaction mechanism, both experiments and density functional theory (DFT) calculations were performed. First, we studied the rotational barriers for the enantiomerization of substrate **1a** and seven-membered bridged biaryl hemiacetal intermediate **1a′**. The computed barrier of substrate **1a** is 34.8 kcal/mol (Fig. 4A), indicating that **1a** cannot enantiomerize directly via rotation about the axial C—C bond under the reaction conditions. Instead, the enantiomerization is feasible through the intermediary of the lower energy pathway involving firstly the conversion of **1a** into hemiacetal **1a′** and the subsequent enantiomerization of **1a′**, which has a barrier of 19.9 or 22.6 kcal/mol (see fig. S4A), depending on the chirality of the hemiacetal carbon (Fig. 4, B and D). This suggests that bridged biaryl intermediate **1a′** is configurational labile under reaction conditions. Since the bridged biaryl hemiacetal intermediate **1a′** is a minor part of an equilibrating mixture (via ring-closing and ring-opening), we cannot determine the rotational barrier experimentally. However, we successfully determined the rotational barrier of the bridged biaryl lactone **4**, which has a similar structure to bridged biaryl hemiacetal intermediate **1a′**. We performed the chiral high-performance liquid chromatography (HPLC) analysis of the lactone **4**. Gratifyingly, a Batman-type chromatogram (*78*) was observed. Subsequently, we submitted this chromatogram to DCXplorer software designed by Schurig group (*79*), and the rotational barrier of lactone **4** was determined as 21.9 kcal/mol (Fig. 4C), which is in excellent agreement with the computed rotational barrier of **4** (22.2 kcal/mol; see fig. S4B). Notably, the rotational barrier of bridged biaryl hemiacetal intermediate **1a′** (19.9 or 22.6 kcal/mol) is slightly lower than the rotational barrier required to isolate the individual atropisomers (24 kcal/mol) (*2*), which demonstrates the great challenge for the DKR via this intermediate. On the basis of the above preliminary results and the x-ray crystal structure of the catalytic adduct **3a**, a possible reaction pathway is proposed in Fig. 4D. The addition of carbene catalyst to aldehyde **2c** forms Breslow intermediate **I**, which after oxidation affords azolium intermediate **II**. Compound *R*-**1a** reacts with acyl azolium intermediate **II** faster than compound *S*-**1a**, and the compound *S*-**1a** is converted to *R*-**1a** by forming the configurationally labile bridged biaryl hemiacetal intermediate **1a′**, thus finally providing the observed *R*-**3c** product in high yield with excellent enantioselectivity.

To elucidate the observed enantioselectivity, DFT calculations were performed, focusing on the key enantio-determining step of this transformation (Fig. 5A). Notably, this step involves the C—O bond formation between hydroxyl group in **1a** and the carbonyl carbon of acyl azolium intermediate **II**. Considering the prochiral nature of the carbonyl carbon in **II**, we examined the key TS structures, allowing attacks from both the *Re*-face and the *Si*-face by the OH group on either *R* or *S* conformers of **1a**. The TS structures for both *Re*- and the *Si*-face attacks of the OH group on either the *R* or *S* conformer of **1a**, along with their relative Gibbs energies are presented in Fig. 5A. For the *R* conformer, the calculated TS barriers for the model reaction reveal that the OH group attack at the carbonyl carbon of the acyl azolium intermediate from the *Si*-face, **TS-*R*-*Si***, is more favorable by 3.5 kcal/mol compared to the *Re*-face, **TS-*R*-*Re***. On the other hand, for the *S* conformer, the computed TS barrier for the attack from the *Re*-face, **TS-*S*-*Re***, is slightly lower in energy by 0.6 kcal/mol compared to the *Si*-face, **TS-*S*-*Si***. Overall, the calculated TS barriers suggest that the acylation of *R*-**1a** via **TS-*R*-*Si*** has a barrier that is 2.9 kcal/mol lower than the acylation of *S*-**1a** via **TS-*S*-*Re***, resulting in a predicted *ee* of 98.5% for the acylated product *R*-**3c**, consistent with the experimentally observed enantioselectivity. **TS-*R*-*Si*** is favored over **TS-*S*-*Re*** primarily because of the former's

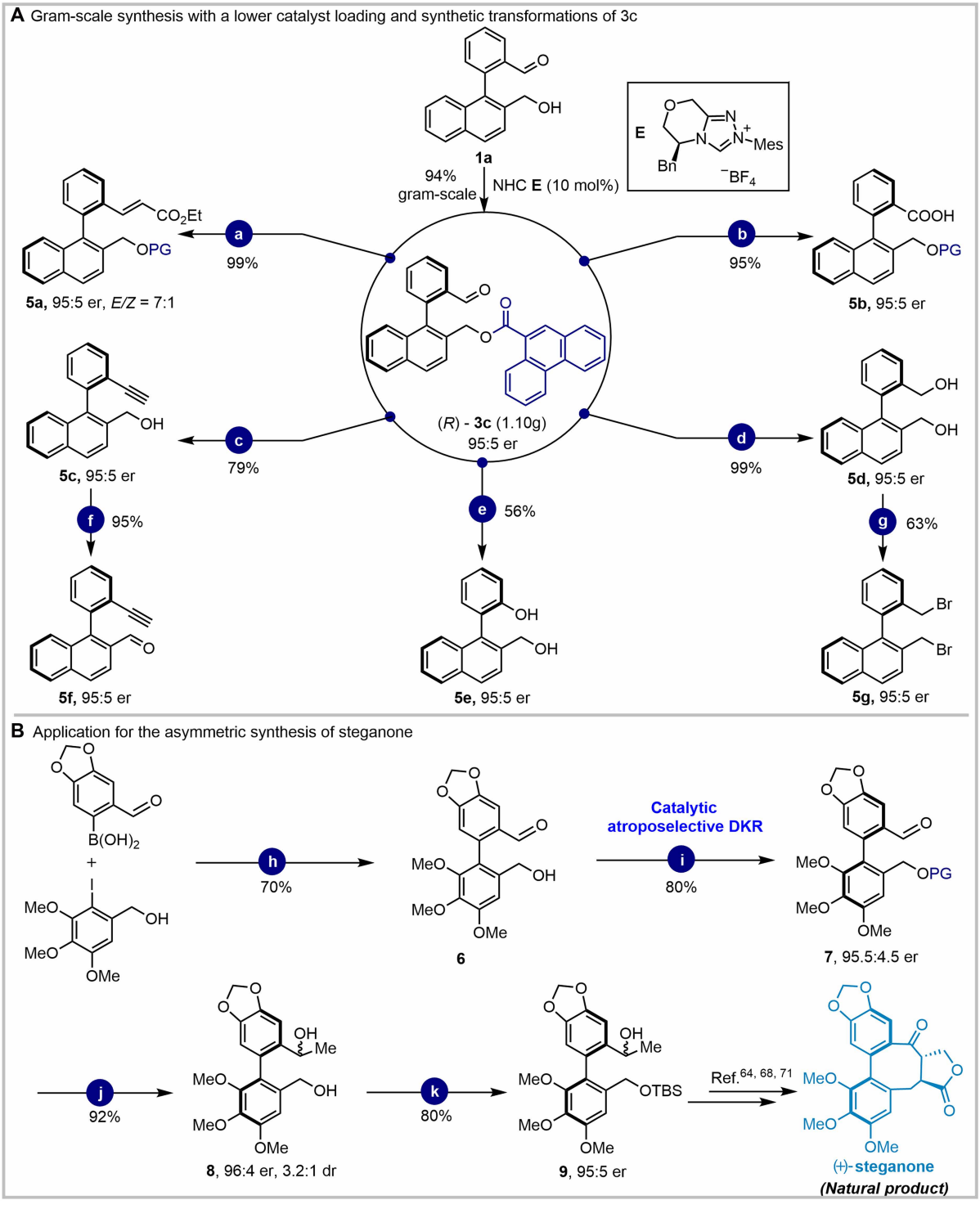

Fig. 3. Synthetic transformations of products and applications in the synthesis of natural product. (**A**) [a]Ethyl (triphenylphosphoranylidene)acetate, CH_2Cl_2, 25°C, 12 hours; [b]$NaClO_2$, NaH_2PO_4, 2-methylbut-2-ene, ^tBuOH, room temperature, overnight; [c]P-(1-diazo-2-oxo-propyl)-dimethylester, K_2CO_3, MeOH, 0°C, 24 hours; [d]$LiAlH_4$, tetrahydrofuran (THF), 0°C, 20 min; [e]m-CPBA, CH_2Cl_2, 0°C to room temperature, 72 hours, then NaOH, MeOH, 2 hours; [f]Dess-Martin periodinane, CH_2Cl_2, 0°C to room temperature, 2 hours; [g]PBr_3, THF, 0°C, 1 hour. (**B**) [h]$Pd(PPh_3)_4$, K_3PO_4, *N*,*N*′-dimethylformamide (DMF), 80°C, 30 hours; [i]NHC·HBF_4 E, LiOH, DQ, 4-Å MS, DCE, room temperature; 7 days; [j]MeLi, THF, −78°C, N_2, 30 min; [k]imidazole, DMAP, TBSCl, DMF, 0°C, N_2, 1 hour.

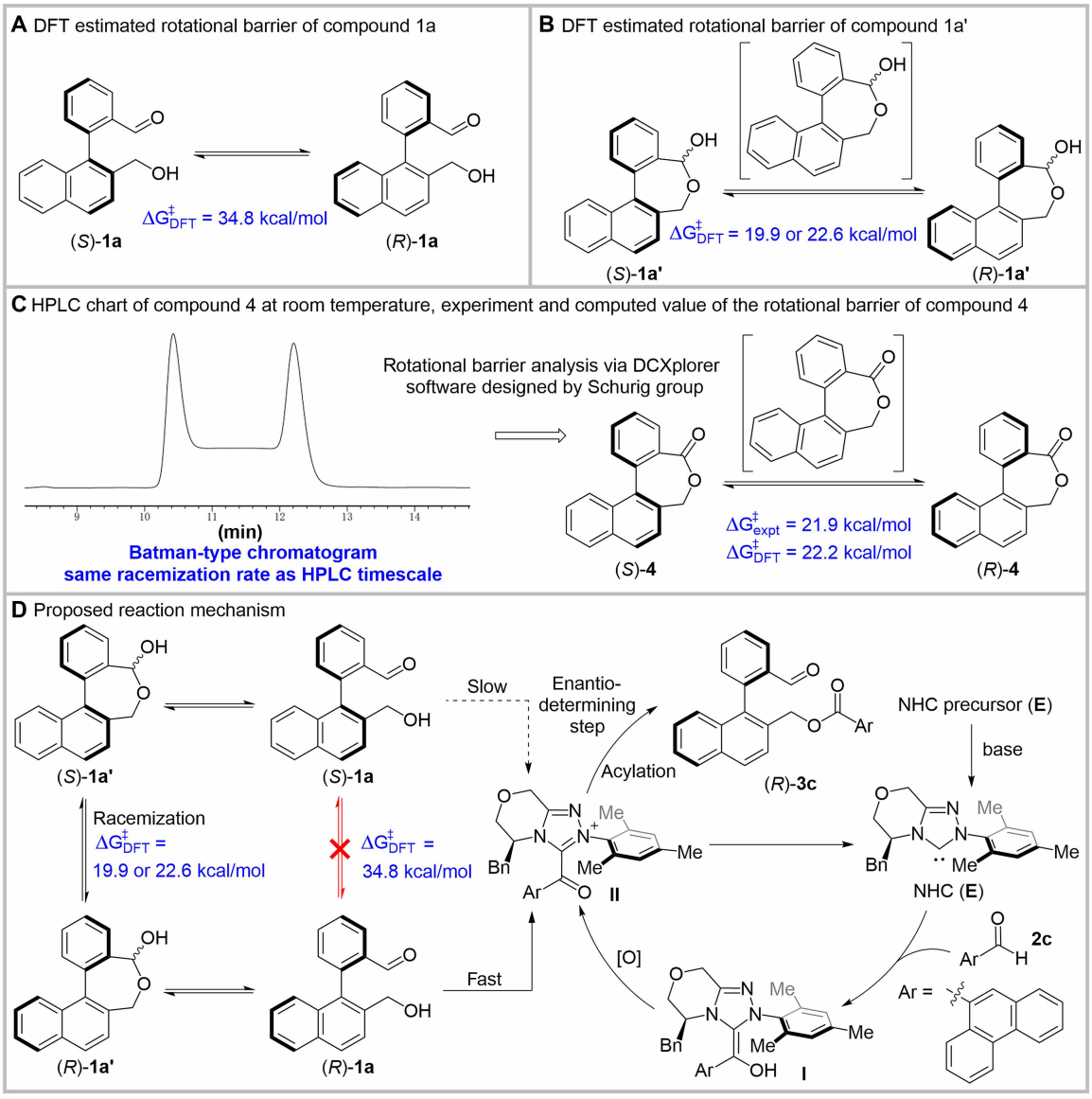

Fig. 4. Determination of the rotational barrier of key compounds and the proposed mechanism. (**A**) DFT estimated rotational barrier of compound 1a. (**B**) DFT estimated rotational barrier of compound 1a′. (**C**) HPLC chart of compound 4 at room temperature, experiment and computed value of the rotational barrier of compound 4. (**D**) Proposed reaction mechanism.

much lower distortion energy (by 18.1 kcal/mol) between the two interacting fragments as they approach each other to form the TS, which more than compensates its less stabilizing (by 14.7 kcal/mol) noncovalent interactions, including π-π and cation-π stacking present in both TSs (fig. S2) (see table S4 in the Supplementary Materials).

In the studied transformation, compound **4** may be produced when the N-heterocyclic carbene (NHC) catalyst react with substrate **1a** to form the acyl azolium intermediate, followed by an intramolecular cyclization reaction. To understand why compound **4** is formed only as a by-product and compound *R*-**3c** is formed as a predominant product (chemoselectivity), we investigated the thermodynamics governing the formation of acyl azolium intermediates **II** (from NHC and **2c**) and **III** (from NHC and **1a,** see SI). Our findings suggest that the formation of **II** ($\Delta G_r = -3.1$ kcal/mol) is more favorable by 2.5 kcal/mol compared to **III** ($\Delta G_r = -0.6$ kcal/mol). In addition, the computed reaction barrier for the C—C bond formation when the NHC carbon atom attacks the carbonyl carbon of substrate **2c** (**TS-2c**; Fig. 5B) is lower by 5.5 kcal/mol than the corresponding barrier when the NHC carbon attacks the carbonyl carbon of substrate **1a** (**TS-1a**; Fig. 5B). Thus, both thermodynamically and kinetically, the formation of product *R*-**3c** is more favored over the formation of compound **4**.

DISCUSSION

In summary, we have developed a carbene-catalyzed dynamic kinetic acylation via the formation of transient bridged biaryl seven-membered cyclic hemiacetals. A series of axially chiral biaryl aldehyde

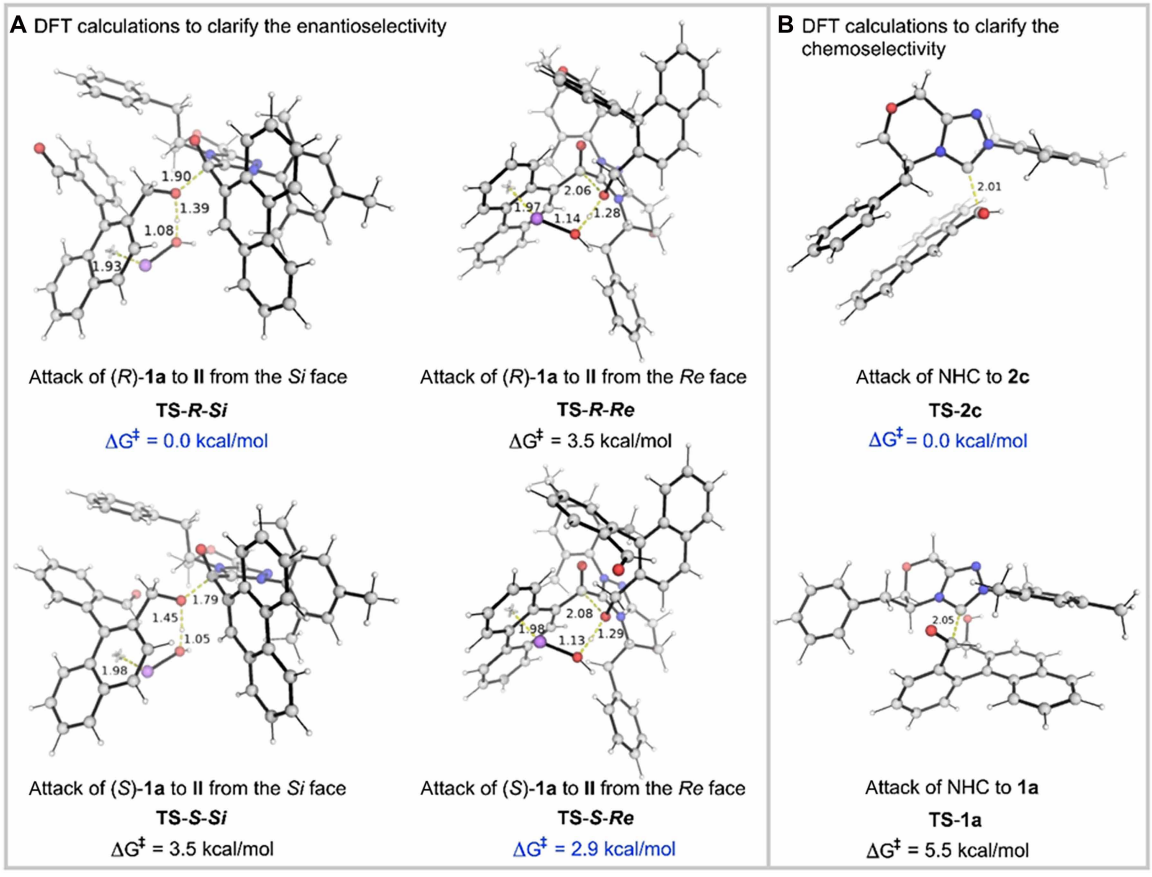

Fig. 5. DFT calculations to clarify the enantio- and chemo-selectivities. (**A**) DFT calculations to clarify the enantioselectivity. (**B**) DFT calculations to clarify the chemoselectivity. Key bond distances are given in Å. Activation barriers are given relative to the lowest activation barrier. Gibbs energies were computed at SMD(DCE)-M06-2X/def2-TZVP//M06-2X/def2-SVP level of theory (see SI for full computational methods).

products were obtained in high yields with excellent enantioselectivities. One of the chiral aldehyde products can be used as the key intermediate for the asymmetric synthesis of steganone. Mechanism studies showed that the key for the success of this DKR reaction is the formation of transient seven-membered cyclic hemiacetals, which has relatively higher rotation barriers yet still is configurational labile under the reaction conditions. We believe that this approach will provide a unique perspective on the development of DKR for the enantioconvergent synthesis of axially chiral compounds.

MATERIALS AND METHODS

General procedure

All reactions were monitored by thin-layer chromatography (TLC). TLC analysis was performed by illumination with an ultraviolet (UV) lamp (254 nm). Anhydrous DCE was purchased from commercial sources, and anhydrous tetrahydrofuran (THF) was distilled from sodium benzophenone ketyl. Anhydrous CH_2Cl_2 and $CHCl_3$ was distilled from CaH_2 under an atmosphere of nitrogen. All flash chromatography was packed with silica gel as the stationary phase. ^{1}H nuclear magnetic resonance (NMR) spectra were recorded on a Bruker (500 and 700 MHz) and JNM-ECZL400S (400 MHz) instrument, and chemical shifts were reported in parts per million (ppm) downfield from internal tetramethylsilane (TMS) with the solvent resonance as the internal standard [$CDCl_3$, δ = 7.26 ppm; dimethyl sulfoxide (DMSO), δ = 2.50 ppm]. ^{13}C NMR spectra were recorded on a Bruker (126 and 176 MHz) and JNM-ECZL400S (101 MHz) instrument, and chemical shifts were reported in parts per million downfield from TMS with the solvent resonance as the internal standard ($CDCl_3$, δ = 77 ppm; DMSO, δ = 39.50 ppm). ^{19}F NMR spectra were recorded on a Bruker (471 and 659 MHz) instrument. Infrared spectra were recorded on a TGA4000 Fourier transform infrared Frontier spectrometer. Optical rotations were measured on a WZZ-2B polarimeter. High-resolution mass spectrometry (MS) analysis was carried out using a time-of-flight MS instrument with an electrospray ionization source. X-ray data were taken on an Agilent SuperNova x-ray diffractometer equipped with a large area charge-coupled device detector. HPLC analysis was performed on Shimadzu SIL-16 with UV detector.

General procedure for the NHC-catalyzed asymmetric reaction

To a dried 4-ml test tube with a stir bar was added the carbene catalyst **E** (20 mol %), substrates **1** (0.1 mmol), **2** (0.12 mmol, 1.2 equiv), 4-Å MS (100 mg), DQ (49.8 mg, 1.2 equiv), anhydrous DCE (2.0 ml) and LiOH (3.0 equiv). The reaction mixture was stirred at room temperature for 3 to 7 days until the starting material disappeared as indicated by TLC and then directly purified by silica gel column chromatography to afford the desired product (*R*)-**3** (*PE*/*EA* = 20:1).

Supplementary Materials

This PDF file includes:

Sections S1 to S7
Tables S1 to S4
Figs. S1 to S7
References

REFERENCES AND NOTES

1. G. Bringmann, A. J. Price Mortimer, P. A. Keller, M. J. Gresser, J. Garner, M. Breuning, Atroposelective synthesis of axially chiral niaryl compounds. *Angew. Chem. Int. Ed.* **44**, 5384–5427 (2005).
2. E. Kumarasamy, R. Raghunathan, M. P. Sibi, J. Sivaguru, Nonbiaryl and heterobiaryl atropisomers: Molecular templates with promise for atropselective chemical transformations. *Chem. Rev.* **115**, 11239–11300 (2015).
3. Y.-B. Wang, B. Tan, Construction of axially chiral compounds via asymmetric organocatalysis. *Acc. Chem. Res.* **51**, 534–547 (2018).
4. J. A. Carmona, C. Rodríguez-Franco, R. Fernández, V. Hornillos, J. M. Lassaletta, Atroposelective transformation of axially chiral (hetero)biaryls. From desymmetrization to modern resolution strategies. *Chem. Soc. Rev.* **50**, 2968–2983 (2021).
5. C.-X. Liu, W.-W. Zhang, S.-Y. Yin, Q. Gu, S.-L. You, Synthesis of atropisomers by transition-metal–catalyzed asymmetric C–H functionalization reactions. *J. Am. Chem. Soc.* **143**, 14025–14040 (2021).
6. G. Bringmann, T. Gulder, T. A. M. Gulder, M. Breuning, Atroposelective total synthesis of axially chiral biaryl natural products. *Chem. Rev.* **111**, 563–639 (2011).
7. J. Wencel-Delord, A. Panossian, F. R. Leroux, F. Colobert, Recent advances and new concepts for the synthesis of axially stereoenriched biaryls. *Chem. Soc. Rev.* **44**, 3418–3430 (2015).
8. J. K. Cheng, S.-H. Xiang, S. Li, L. Ye, B. Tan, Recent advances in catalytic asymmetric construction of atropisomers. *Chem. Rev.* **121**, 4805–4902 (2021).
9. H.-H. Zhang, F. Shi, Organocatalytic atroposelective synthesis of indole derivatives bearing axial chirality: Strategies and applications. *Acc. Chem. Res.* **55**, 2562–2580 (2022).
10. C. B. Roos, C.-H. Chiang, L. A. M. Murray, D. Yang, L. Schulert, A. R. H. Narayan, Stereodynamic strategies to induce and enrich chirality of atropisomers at a late stage. *Chem. Rev.* **123**, 10641–10727 (2023).
11. S.-H. Xiang, W.-Y. Ding, Y.-B. Wang, B. Tan, Catalytic atroposelective synthesis. *Nat. Catal.* **7**, 483–498 (2024).
12. X. Zhang, K. Zhao, Z. Gu, Transition metal-catalyzed biaryl atropisomer synthesis via a torsional strain promoted ring-opening reaction. *Acc. Chem. Res.* **55**, 1620–1633 (2022).
13. J. Q. Shi, F. Fang, D.-J. Cheng, Organocatalytic atroposelective dynamic kinetic resolution involving ring manipulations. *Adv. Synth. Catal.* **366**, 1269–1284 (2024).
14. J. A. Carmona, C. Rodríguez-Franco, R. Fernández, J. M. Lassaletta, V. Hornillos, Lewis acid-base interactions as a racemization strategy for the atroposelective synthesis of (hetero)biaryls via dynamic kinetic resolution. *ChemCatChem* **16**, e202400701 (2024).
15. C. Wu, Y. Jin, X. Zhang, R. Gao, X. Dou, Development of configurationally labile biaryl reagents for atropisomer synthesis. *Eur. J. Org. Chem.* **27**, e202400402 (2024).
16. S. E. Huth, E. A. Stone, S. Crotti, S. J. Miller, On the ability of the N—O bond to support a stable stereogenic axis: Peptide-catalyzed atroposelective N-oxidation. *J. Org. Chem.* **88**, 12857–12862 (2023).
17. K. Zhao, L. Duan, S. Xu, J. Jiang, Y. Fu, Z. Gu, Enhanced reactivity by torsional strain of cyclic diaryliodonium in Cu-catalyzed enantioselective ring-opening reaction. *Chem* **4**, 599–612 (2018).
18. S. Yang, T. Zheng, L. Duan, X. Xue, Z. Gu, Atroposelective three-component coupling of cyclic diaryliodoniums and sodium cyanate enabled by the dual-role of phenol. *Angew. Chem. Int. Ed. Engl.* **62**, e202302749 (2023).
19. J. Han, B. Xiao, T.-Y. Sun, M. Wang, L. Jin, W. Yu, Y. Wang, D.-M. Fang, Y. Zhou, X.-F. Wu, Y.-D. Wu, J. Liao, Enantioselective double carbonylation enabled by high-valent palladium catalysis. *J. Am. Chem. Soc.* **144**, 21800–21807 (2022).
20. J. Zhang, T. Sun, Z. Zhang, H. Cao, Z. Bai, Z.-C. Cao, Nickel-catalyzed enantioselective arylative activation of aromatic C–O bond. *J. Am. Chem. Soc.* **143**, 18380–18387 (2021).
21. L. Pang, Q. Sun, Z. Huang, G. Li, J. Liu, J. Guo, C. Yao, J. Yu, Q. Li, Palladium-catalyzed stereoselective cleavage of C—P bond: Enantioselective construction of atropisomers containing a P-stereogenic center. *Angew. Chem. Int. Ed. Engl.* **61**, e202211710 (2022).
22. M. Wu, Y.-W. Chen, Q. Lu, Y.-B. Wang, J. K. Cheng, P. Yu, B. Tan, Organocatalytic Si–C aryl bond functionalization-enabled atroposelective synthesis of axially chiral biaryl siloxanes. *J. Am. Chem. Soc.* **145**, 20646–20654 (2023).
23. Y. Liu, Y.-L. S. Tse, F. Y. Kwong, Y.-Y. Yeung, Accessing axially chiral biaryls via organocatalytic enantioselective dynamic-kinetic resolution-semipinacol rearrangement. *ACS Catal.* **7**, 4435–4440 (2017).
24. Z. Zhang, J. Zhang, Q. Gao, Y. Zhou, M. Yang, H. Cao, T. Sun, G. Luo, Z.-C. Cao, Enantioselective alkylative cross-coupling of unactivated eromatic C–O electrophiles. *Nat. Commun.* **13**, 2953 (2022).
25. G. Bringmann, T. Hartung, First atropo-enantioselective ring opening of achiral biaryls containing lactone bridges with chiral hydride-transfer reagents derived from borane. *Angew. Chem. Int. Ed. Engl.* **31**, 761–762 (1992).
26. G.-Q. Chen, B.-J. Lin, J.-M. Huang, L.-Y. Zhao, Q.-S. Chen, S.-P. Jia, Q. Yin, X. Zhang, Design and synthesis of chiral oxa-spirocyclic ligands for Ir-catalyzed direct asymmetric reduction of Bringmann's lactones with molecular H_2. *J. Am. Chem. Soc.* **140**, 8064–8068 (2018).
27. C. Yu, H. Huang, X. Li, Y. Zhang, W. Wang, Dynamic kinetic resolution of biaryl lactones via a chiral bifunctional amine thiourea-catalyzed highly atropo-enantioselective transesterification. *J. Am. Chem. Soc.* **138**, 6956–6959 (2016).
28. O. M. Beleh, E. Miller, F. D. Toste, S. J. Miller, Catalytic dynamic kinetic resolutions in tandem to construct two-axis terphenyl atropisomers. *J. Am. Chem. Soc.* **142**, 16461–16470 (2020).
29. Z. H. Luo, W. T. Wang, T. Y. Tang, S. Zhang, F. Huang, D. Hu, L. F. Tao, L. Qian, J. Y. Liao, Torsional strain-independent catalytic enantioselective synthesis of biaryl atropisomers. *Angew. Chem. Int. Ed. Engl.* **61**, e202211303 (2022).
30. G. Wang, Q. Shi, W. Hu, T. Chen, Y. Guo, Z. Hu, M. Gong, J. Guo, D. Wei, Z. Fu, W. Huang, Organocatalytic asymmetric *N*-sulfonyl amide C-N bond activation to access axially chiral biaryl amino acids. *Nat. Commun.* **11**, 946 (2020).
31. Y. Cai, Y. Zhao, K. Tang, H. Zhang, X. Mo, J. Chen, Y. Huang, Amide C–N bonds activation by A new variant of bifunctional N-heterocyclic carbene. *Nat. Commun.* **15**, 496 (2024).
32. Y. Yang, C. Wu, J. Xing, X. Dou, Developing biarylhemiboronic esters for biaryl atropisomer synthesis via dynamic kinetic atroposelective Suzuki–Miyaura cross-coupling. *J. Am. Chem. Soc.* **146**, 6283–6293 (2024).
33. L. Wei, J. Li, Y. Zhao, Q. Zhou, Z. Wei, Y. Chen, X. Zhang, X. Yang, Chiral phosphoric acid catalyzed asymmetric hydrolysis of biaryl oxazepines for the synthesis of axially chiral biaryl amino phenol derivatives. *Angew. Chem. Int. Ed. Engl.* **62**, e202306864 (2023).
34. V. Hornillos, J. A. Carmona, A. Ros, J. Iglesias-Sigüenza, J. López-Serrano, R. Fernández, J. M. Lassaletta, Dynamic kinetic resolution of heterobiaryl ketones by zinc-catalyzed asymmetric hydrosilylation. *Angew. Chem. Int. Ed. Engl.* **57**, 3777–3781 (2018).
35. Y.-D. Shao, J.-S. Feng, D.-D. Han, K.-H. Pan, L. Zhang, Y.-F. Wang, Z.-H. Ma, P.-R. Wang, M. Yin, D.-J. Cheng, Construction of axially chiral styrene-type allylamines via chiral phosphoric acid-catalyzed asymmetric reductive amination. *Org. Chem. Front.* **9**, 764–770 (2022).
36. H. X. Jiang, D. D. Han, R. P. Song, Q. Shi, X. F. He, W. Q. Kou, Q. Zhao, Y. D. Shao, D. J. Cheng, Chiral boro-phosphate catalyzed asymmetric transfer hydrogenation of 1-enal substituted 2-naphthols: Access to axially chiral styrene-type allylalcohols. *Adv. Synth. Catal.* **365**, 1398–1404 (2023).
37. F. Guo, S. Fang, J. He, Z. Su, T. Wang, Enantioselective organocatalytic synthesis of axially chiral aldehyde-containing styrenes via SNAr reaction-guided dynamic kinetic resolution. *Nat. Commun.* **14**, 5050 (2023).
38. K. Mori, T. Itakura, T. Akiyama, Enantiodivergent atroposelective synthesis of chiral biaryls by asymmetric transfer hydrogenation: Chiral phosphoric acid catalyzed dynamic kinetic resolution. *Angew. Chem. Int. Ed. Engl.* **55**, 11642–11646 (2016).
39. J. Zhang, J. Wang, Atropoenantioselective redox-neutral amination of biaryl compounds through borrowing hydrogen and dynamic kinetic resolution. *Angew. Chem. Int. Ed. Engl.* **57**, 465–469 (2018).
40. D. Guo, J. Zhang, B. Zhang, J. Wang, Ruthenium-catalyzed atropoenantioselective synthesis of axial biaryls via reductive amination and dynamic kinetic resolution. *Org. Lett.* **20**, 6284–6288 (2018).
41. D. Guo, Q. Peng, B. Zhang, J. Wang, Atroposelective dynamic kinetic resolution via in situ hemiaminals catalyzed by *N*-heterocyclic carbene. *Org. Lett.* **23**, 7765–7770 (2021).
42. J. A. Carmona, C. Rodríguez-Franco, J. López-Serrano, A. Ros, J. Iglesias-Sigüenza, R. Fernández, J. M. Lassaletta, V. Hornillos, Atroposelective transfer hydrogenation of biaryl aminals via dynamic kinetic resolution. Synthesis of axially chiral diamines. *ACS Catal.* **11**, 4117–4124 (2021).
43. Y. Lv, G. Luo, Q. Liu, Z. Jin, X. Zhang, Y. R. Chi, Catalytic atroposelective synthesis of axially chiral benzonitriles via chirality control during bond dissociation and CN group formation. *Nat. Commun.* **13**, 36 (2022).
44. Z. Zheng, Q. Liu, X. Peng, Z. Jin, J. Wu, NHC-catalyzed chemo- and enantioselective reaction between aldehydes and enals for access to axially chiral arylaldehydes. *Org. Lett.* **26**, 917–921 (2024).
45. X. Hao, Z. Tian, Z. Yao, T. Zang, S. Song, L. Lin, T. Qiao, L. Huang, H. Fu, Atroposelective synthesis of axial biaryls by dynamic kinetic resolution using engineered imine reductases. *Angew. Chem. Int. Ed. Engl.* **63**, e202410112 (2024).
46. S. Staniland, R. W. Adams, J. J. W. McDouall, I. Maffucci, A. Contini, D. M. Grainger, N. J. Turner, J. Clayden, Biocatalytic dynamic kinetic resolution for the synthesis of atropisomeric biaryl *N*-oxide Lewis base catalysts. *Angew. Chem. Int. Ed. Engl.* **55**, 10755–10759 (2016).
47. X. Yuan, J. Wang, Atropoenantioselective synthesis of heterobiaryl *N*-oxides via dynamic kinetic resolution. *Sci. Chin. Chem.* **65**, 2512–2516 (2022).
48. J. A. Carmona, P. Rodríguez-Salamanca, R. Fernández, J. M. Lassaletta, V. Hornillos, Dynamic kinetic resolution of 2-(Quinolin-8-yl) benzaldehydes: Atroposelective

iridium-catalyzed transfer hydrogenative allylation. *Angew. Chem. Int. Ed. Engl.* **62**, e202306981 (2023).
49. P. Rodríguez-Salamanca, G. de Gonzalo, J. A. Carmona, J. López-Serrano, J. Iglesias-Sigüenza, R. Fernández, J. M. Lassaletta, V. Hornillos, Biocatalytic atroposelective synthesis of axially chiral *N*-arylindoles via dynamic kinetic resolution. *ACS Catal.* **13**, 659–664 (2023).
50. C. Rodríguez-Franco, A. Ros, P. Merino, R. Fernández, J. M. Lassaletta, V. Hornillos, Dynamic kinetic resolution of indole-based sulfenylated heterobiaryls by rhodium-catalyzed atroposelective reductive aldol reaction. *ACS Catal.* **13**, 12134–12141 (2023).
51. C. Rodríguez-Franco, E. Roldán-Molina, A. Aguirre-Medina, R. Fernández, V. Hornillos, J. M. Lassaletta, Catalytic atroposelective synthesis of C–N axially chiral aminophosphines via dynamic kinetic resolution. *Angew. Chem. Int. Ed. Engl.* **63**, e202409524 (2024).
52. J. M. Coto-Cid, V. Hornillos, R. Fernández, J. M. Lassaletta, G. de Gonzalo, Chemoenzymatic dynamic kinetic resolution of atropoisomeric 2-(Quinolin-8-yl)benzylalcohols. *J. Org. Chem.* **90**, 5120–5124 (2025).
53. N. Kotwal, Tamanna, P. Chauhan, Catalytic asymmetric synthesis of medium-sized bridged biaryls. *Chem. Commun.* **58**, 11031–11044 (2022).
54. X. Yang, L. Wei, Y. Wu, L. Zhou, X. Zhang, Y. R. Chi, Atroposelective access to 1, 3-oxazepine-containing bridged biaryls via carbene-catalyzed desymmetrization of imines. *Angew. Chem. Int. Ed. Engl.* **62**, e202211977 (2023).
55. Z. Wei, Y. Zhao, T. Wang, J. Li, W. Yuan, L. Wei, X. Yang, Bridged biaryl atropisomers by organocatalyzed kinetic asymmetric alcoholysis. *Org. Lett.* **26**, 7110–7115 (2024).
56. X. Bugaut, F. Glorius, Organocatalytic umpolung: *N*-heterocyclic carbenes and beyond. *Chem. Soc. Rev.* **41**, 3511–3522 (2012).
57. S. J. Ryan, L. Candish, D. W. Lupton, Acyl anion free *N*-heterocyclic carbene organocatalysis. *Chem. Soc. Rev.* **42**, 4906–4917 (2013).
58. D. M. Flanigan, F. Romanov-Michailidis, N. A. White, T. Rovis, Organocatalytic reactions enabled by *N*-heterocyclic carbenes. *Chem. Rev.* **115**, 9307–9387 (2015).
59. K. J. R. Murauski, A. A. Jaworski, K. A. Scheidt, A continuing challenge: N-heterocyclic carbene-catalyzed syntheses of γ-butyrolactones. *Chem. Soc. Rev.* **47**, 1773–1782 (2018).
60. S. Mondal, S. R. Yetra, S. Mukherjee, A. T. Biju, NHC-catalyzed generation of α,β-unsaturated acylazoliums for the enantioselective synthesis of heterocycles and carbocycles. *Acc. Chem. Res.* **52**, 425–436 (2019).
61. X.-Y. Chen, Z.-H. Gao, S. Ye, Bifunctional *N*-heterocyclic carbenes derived from l-pyroglutamic acid and their applications in enantioselective organocatalysis. *Acc. Chem. Res.* **53**, 690–702 (2020).
62. R. Song, Y. Xie, Z. Jin, Y. R. Chi, Carbene-catalyzed asymmetric construction of atropisomers. *Angew. Chem. Int. Ed. Engl.* **60**, 26026–26037 (2021).
63. K. M. Meragelman, T. C. McKee, M. R. Boyd, 10-Demethoxystegane, A new lignan from *Steganotaenia araliacea*. *J. Nat. Prod.* **64**, 1480–1482 (2001).
64. A. I. Meyers, J. R. Flisak, R. A. Aitken, Asymmetric synthesis of (−)-steganone. Further application of chiral biaryl syntheses. *J. Am. Chem. Soc.* **109**, 5446–5452 (1987).
65. H. Abe, S. Takeda, T. Fujita, K. Nishioka, Y. Takeuchi, T. Harayama, Enantioselective construction of biaryl part in the synthesis of stegane related compounds. *Tetrahedron Lett.* **45**, 2327–2329 (2004).
66. L. G. Monovich, Y. Le Huérou, M. Rönn, G. A. Molander, Total synthesis of (−)-steganone utilizing a samarium(II) iodide promoted 8-endo ketyl–olefin cyclization. *J. Am. Chem. Soc.* **122**, 52–57 (2000).
67. K. Kamikawa, T. Watanabe, A. Daimon, M. Uemura, Stereoselective synthesis of axially chiral natural products, (−)-steganone and O,O′-dimethylkorupensamine A, utilizing planar chiral (Arene)chromium complexes. *Tetrahedron* **56**, 2325–2337 (2000).
68. M. Uemura, A. Daimon, Y. Hayashi, An asymmetric synthesis of an axially chiral biaryl via an (Arene)chromium complex: Formal synthesis of (−)-steganone. *J. Chem. Soc. Chem. Commun.* **1995**, 1943–1944 (1995).
69. B. Yalcouye, S. Choppin, A. Panossian, F. R. Leroux, F. Colobert, A concise atroposelective formal synthesis of (–)-steganone. *Eur. J. Org. Chem.* **2014**, 6285–6294 (2014).
70. Q. Dherbassy, J. Wencel-Delord, F. Colobert, Asymmetric C–H activation as a modern strategy towards expedient synthesis of steganone. *Tetrahedron* **72**, 5238–5245 (2016).
71. S. Takeda, H. Abe, Y. Takeuchi, T. Harayama, Intramolecular biaryl coupling reaction of benzyl benzoate and phenyl benzoate derivatives, and its application to the formal synthesis of (−)-steganone. *Tetrahedron* **63**, 396–408 (2007).
72. S. De Sarkar, S. Grimme, A. Studer, NHC catalyzed oxidations of aldehydes to esters: Chemoselective acylation of alcohols in presence of amines. *J. Am. Chem. Soc.* **132**, 1190–1191 (2010).
73. M. He, J. R. Struble, J. W. Bode, Highly enantioselective azadiene Diels–Alder reactions catalyzed by chiral *N*-heterocyclic carbenes. *J. Am. Chem. Soc.* **128**, 8418–8420 (2006).
74. S. P. Lathrop, T. Rovis, A photoisomerization-coupled asymmetric stetter reaction: Application to the total synthesis of three diastereomers of (−)-cephalimysin A. *Chem. Sci.* **4**, 1668–1673 (2013).
75. M. S. Kerr, T. Rovis, Enantioselective synthesis of quaternary stereocenters via a catalytic asymmetric stetter reaction. *J. Am. Chem. Soc.* **126**, 8876–8877 (2004).
76. P.-C. Chiang, M. Rommel, J. W. Bode, α′-Hydroxyenones as mechanistic probes and scope-expanding surrogates for α,β-unsaturated aldehydes in *N*-heterocyclic carbene-catalyzed reactions. *J. Am. Chem. Soc.* **131**, 8714–8718 (2009).
77. M. Wadamoto, E. M. Phillips, T. E. Reynolds, K. A. Scheidt, Enantioselective synthesis of α,α-disubstituted cyclopentenes by an *N*-heterocyclic carbene-catalyzed desymmetrization of 1,3-diketones. *J. Am. Chem. Soc.* **129**, 10098–10099 (2007).
78. J.-P. Heeb, J. Clayden, M. D. Smith, R. J. Armstrong, R. J., Interrogating the configurational stability of atropisomers. *Nat. Protoc.* **18**, 2745–2771 (2023).
79. O. Trapp, G. Schoetz, V. Schurig, V., Determination of enantiomerization barriers by dynamic and stopped-flow chromatographic methods. *Chirality* **13**, 403–414 (2001).
80. S. Shee, S. Shree Ranganathappa, M. S. Gadhave, R. Gogoi, A. T. Biju, Enantioselective synthesis of C–O axially chiral diaryl ethers by NHC-catalyzed atroposelective desymmetrization. *Angew. Chem. Int. Ed. Engl.* **62**, e202311709 (2023).
81. Y. Wu, X. Guan, H. Zhao, M. Li, T. Liang, J. Sun, G. Zheng, Q. Zhang, Synthesis of axially chiral diaryl ethers via NHC-catalyzed atroposelective esterification. *Chem. Sci.* **15**, 4564–4570 (2024).
82. A. Rosales Martínez, L. Enríquez, M. Jaraíz, L. Pozo Morales, I. Rodríguez-García, E. Díaz Ojeda, A concise route for the synthesis of tetracyclic meroterpenoids: (±)-Aureol preparation and mechanistic interpretation. *Mar. Drugs* **18**, 441 (2020).
83. L. Ding, X. Sui, Z. Gu, Enantioselective synthesis of biaryl atropisomers via Pd/norbornene-catalyzed three-component cross-couplings. *ACS Catal.* **8**, 5630–5635 (2018).
84. S. S. Moleele, J. P. Michael, C. B. de Koning, Tetralones as precursors for the synthesis of 2,2′-disubstituted 1,1′-binaphthyls and related compounds. *Tetrahedron* **64**, 10573–10580 (2008).
85. Y. Zhao, D. G. Truhlar, The M06 suite of density functionals for main group thermochemistry, thermochemical kinetics, noncovalent interactions, excited states, and transition elements: Two new functionals and systematic testing of four M06-class functionals and 12 other functionals. *Theor. Chem. Acc.* **120**, 215–241 (2008).
86. F. Weigend, R. Ahlrichs, Balanced basis sets of split valence, triple zeta valence and quadruple zeta valence quality for H to Rn: Design and assessment of accuracy. *Phys. Chem. Chem. Phys.* **7**, 3297–3305 (2005).
87. F. Weigend, Accurate Coulomb-fitting basis sets for H to Rn. *Phys. Chem. Chem. Phys.* **8**, 1057–1065 (2006).
88. A. V. Marenich, C. J. Cramer, D. G. Truhlar, Universal solvation model based on solute electron density and on a continuum model of the solvent defined by the bulk dielectric constant and atomic surface tensions. *J. Phys. Chem. B* **113**, 6378–6396 (2009).
89. S. Grimme, Supramolecular binding thermodynamics by dispersion-corrected density functional theory. *Chem. A Eur. J.* **18**, 9955–9964 (2012).
90. J. Contreras-García, E. R. Johnson, S. Keinan, R. Chaudret, J.-P. Piquemal, D. N. Beratan, W. Yang, NCIPLOT: A program for plotting noncovalent interaction regions. *J. Chem. Theory Comput.* **7**, 625–632 (2011).

Acknowledgments
Funding: We acknowledge the National Natural Science Foundation of China (22201071), Natural Science Foundation of Hunan Province (2023JJ10027), Scientific Research Fund of Hunan Provincial Education Department (22A0048), and Science and Technology Planning Project of Hunan Province (2018TP1017). X.Z. acknowledges the support from the Agency for Science, Technology, and Research (A*STAR) under its Career Development Fund (CDF Project Number C210812008) and Manufacturing, Trade, and Connectivity (MTC) Young Individual Research Grants (YIRG grant number M22K3c0091) and the Chinese University of Hong Kong for the Vice-Chancellor Early Career Professorship Scheme Research Startup Fund (Project Code 4933634) and Research Startup Matching Support (project code 5501779) for this work.
Author contributions: X.Y. conceptualized and directed this research; S.V.C.V. and X.Z. performed the computational studies and analyzed the results; Q.Z., Y.C., and W.Y. performed the main methodology development, scope evaluation, and synthetic application; X.X. and B.Z. prepared the substrates; and Y.R.C. contributed to discussions and manuscript preparation. **Competing interests:** The authors declare that they have no competing interests. **Data and materials availability:** Geometries of all optimized structures (in .xyz format with their associated energy in Hartrees) are included in a separate folder named DFT_optimized_structures. All these data have been deposited and uploaded to https://zenodo.org/records/15774233 (DOI: 10.5281/zenodo.15774233). Deposition number 2371752 (**3a**) contains the supplementary crystallographic data for this paper. These data can be obtained free of charge from the Cambridge Crystallographic Data Centre. All other data needed to evaluate the conclusions in the paper are present in the paper and/or the Supplementary Materials.

Submitted 29 March 2025
Accepted 2 September 2025
Published 3 October 2025
10.1126/sciadv.adx8255